

## Geochemical Properties and the Nature of Kaolin and Iron Oxides in Upland Oxisols and Ultisols under a Tropical Monsoonal Climate, Thailand

**T. Darunsontaya<sup>1</sup>, A. Sudhiprakarn<sup>1,\*</sup>, I. Kheoruenromne<sup>1</sup> and R.J. Gilkes<sup>2</sup>**

<sup>1</sup>*Department of Soil Science, Faculty of Agriculture, Kasetsart University, Bangkok 10900, Thailand*

<sup>2</sup>*School of Earth and Environment, Faculty of Natural and Agricultural Sciences, University of Western Australia, Crawley, WA 6009, Australia*

*\*Corresponding author. Email: agrals@ku.ac.th*

### **Abstract**

Fifty samples from genetic horizons of 17 soils on various parent materials under a tropical monsoonal climate in Thailand were analyzed for chemical and mineralogical properties of the clay-sized minerals. These Oxisols and Ultisols have kaolinite as the dominant clay mineral and various amounts of accessory minerals with higher amounts of sesquioxide minerals in Oxisols. The crystal size of kaolinite and iron oxides is smaller for basaltic soils relative to soils on granite and sedimentary rocks. Halloysite tubes occur in some soil clays particularly for basaltic soils and these soils also contain gibbsite. Oxisols derived from basalt have relatively higher contents of Fe, Ti, Mg, Mn, Ba, Be, Bi, Ce, Co, Cr, Cu, Ga, La, Nd, Ni, Sc, Sr and Zn. Statistical analysis indicates a lithosequence where soil parent material is the main factor influencing the mineralogical and chemical properties of the clay fraction of these soils.

**Keywords:** kaolinite, goethite, hematite, geochemistry, clay minerals, lithosequence

### **Introduction**

A monsoonal climate occurs in the Peninsula and Southeast Coast zone of Thailand (Yoothong et al., 1997). The high rainfall and temperature in this zone result in intense leaching conditions for upland soils and high weathering rates for many soil minerals. Consequently, kaolin group minerals (mostly disordered kaolinite and halloysite) and sesquioxides (particularly gibbsite, hematite and goethite) are dominant in the clay fraction of these soils (Eswaran and Wong, 1978). Most upland soils in this region are Ultisols and Oxisols with this monotonous mineralogy due to their maturity (Schwertmann and Herbillon, 1992). However, the amounts and properties of clay-sized minerals may vary with parent material, degree of weathering and pedogenic environment (Kanket et al., 2005; Watanabe et al., 2006). The chemical and morphological properties of these minerals particular crystallinity

(structural order), chemical composition and crystal size vary considerably and may affect cation exchange capacity (CEC), specific surface area (SSA) and other soil properties that relate to soil fertility (Hughes and Brown, 1979; Hart et al., 2003). The surface charge properties of these soils relate closely to the nature of kaolin group minerals and sesquioxides (Wisawapipat, 2009). Appropriate soil management requires an understanding of clay fraction mineralogy to provide a basis for developing appropriate management procedures. The research described in this publication is aimed at providing this better understanding of Thai upland soils.

### **Materials and Methods**

#### **Soil Preparation**

One hundred and twenty seven of bulk soil samples were collected from 17 profiles of upland Oxisols and Ultisols in Thailand. These soils

develop on various parent materials (basalt, granite, limestone, various sediments) under a tropical monsoonal climate.

Pedological characteristic of the soils are provided in Table 1. The soil samples were dried and passed through a 2 mm sieve. The representative selected 50 clay fraction samples from genetic horizons of each soil profile were separated from bulk soil samples by removal of organic carbon using H<sub>2</sub>O<sub>2</sub> then the samples were dispersed by stirring and shaking using sodium hexametaphosphate as a dispersing agent. The suspended samples were fractionated into

particle size classes by sedimentation method (Gee and Baulder, 1986). Free iron oxides were removed from all clay fractions by dithionite-citrate-bicarbonate treatment following the procedure of Mehra and Jackson (1960). The deferrated clay samples consisted almost entirely of kaolin group minerals and will henceforth be referred to as kaolins or kaolin concentrates in this paper. Iron oxide in the clay fractions from 15 representative samples from each profile were concentrated by 5M NaOH digestion to remove kaolin and gibbsite (Singh and Gilkes, 1991).

**Table 1** Pedological characteristics of Thai upland Oxisols and Ultisols.

Soil series	Classification	Parent material	Physiographic position	Drainage	Rainfall/ temperature <sup>1/</sup>
<i>Oxisols</i>					
Ao Luek1 (Ak1)	Typic Kandiudox	Residuum from limestone	Karst corrosion plain	Well drained	1883 mm/ 27°C
Ao Luek2 (Ak2)	Rhodic Kandiudox	Residuum from limestone	Rise crestal slope in karst corrosion plain	Well drained	1883 mm/ 27°C
Pathiu (Ptu)	Kandiudalfic Eutrudox	Residuum/colluvium from clastic rocks and limestone	Footslope in karst corrosion plain	Well drained	1883 mm/ 27°C
Tha Mai1 (Ti1)	Rhodic Kandiudox	Residuum from weathered basalt	Upper dissected footslope of lava corrosion hill	Well drained	3330 mm/ 27°C
Tha Mai2 (Ti2)	Typic Kandiudox	Residuum from weathered basalt	Top of dissected lava corrosion plain	Well drained	3330 mm/ 27°C
Tha Mai3 (Ti3)	Typic Kandiudox	Residuum from weathered basalt	Upper footslope of lava corrosion hill	Well drained	3330 mm/ 27°C
Nong Bon1 (Nb1)	Typic Kandiudox	Residuum from weathered basalt	Shoulder slope on lava corrosion undulating plain	Well drained	3524 mm/ 27°C
Nong Bon2 (Nb2)	Typic Kandiudox	Residuum from weathered basalt	Shoulder slope on lava corrosion rolling plain	Well drained	3524 mm/ 27°C
<i>Ultisols</i>					
Kohong (Kh)	Typic Kandiudult	Colluvium derived from weathered sandstone	Shoulder spur hill slope	Well drained	1883 mm/27°C
Khlong Chak (Kc)	Typic Paleudult	Wash and local alluvium from metasediments	Dissected lower residual footslope	Well drained	1803 mm/ 27°C
Fang Daeng (Fd)	Typic Kandiudult	Residuum from clastic sedimentary rocks	Crestal slope of low hill	Well drained	1883 mm/ 27°C
Krabi (Kbi)	Typic Kandiudult	Residuum and colluvium from clastic rocks	Shoulder slope of low hill	Well drained	2171 mm/ 28°C
Sadao (Sd)	Typic Kandiudult	Local alluvium from clastic sedimentary rocks	High local alluvial terrace	Well drained	1883 mm/ 27°C
Phuket (Pk)	Typic Plinthudult	Residuum from weathered granite	Dissected lower footslope	Well drained	3330 mm/ 27°C
Phang-nga (Pga)	Typic Kandiudult	Wash and residuum from weathered granite	Lower coalescing	Well drained	1803 mm/ 27°C
Thai Muang (Tim)	Typic Kandiudult	Wash over residuum from weathered granite	Upper dissected footslope	Well drained	1351 mm/ 26°C
Huai Pong (Hp)	Typic Kandiudult	Residuum from weathered granite	Lower midslope of residual hill	Well drained	1329 mm/ 27°C

<sup>1/</sup> Mean annual value.

## Laboratory Analyses

Whole soil samples were analyzed for physical and chemical properties using standard methods (National Soil Survey Center, 1996). The particle size distribution was determined by the pipette method. Soil pH was measured in 1:1 soil:solution using H<sub>2</sub>O and 1M KCl. Organic carbon was determined by the Walkley and Black method and is expressed as organic matter (OM). Extractable acidity (EA) was measured using barium chloride-triethanolamine buffered at pH 8.2. Cation exchange capacity (CEC) was measured using NH<sub>4</sub>OAc at pH 7.0. The cation exchange capacity of the clay samples and kaolin concentrates were measured using 0.01 M silver thiourea solution at pH 4.7 to displace the exchangeable cations (Rayment and Higginson, 1992). Specific surface area (SSA) was measured using the N<sub>2</sub>-BET method (Aylmore et al., 1970) with a Micrometric Gemini III 2375 surface analyzer.

## Chemical Composition of Clay and Kaolin Concentrates

Major elements of clay samples and kaolin concentrates were determined using a Philips PW1400 XRF spectrometer. Samples were fused with lithium metatetraborate flux at 1050 °C (Norrish and Hutton, 1969). The elemental composition was calculated using a matrix correction procedure and validated by comparison with analyses of certified reference materials. Minor elements in clay samples were determined using an inductively coupled plasma mass spectrometer (Perkin Elmer ICP-MS) after digestion in concentrated HCl and HNO<sub>3</sub>.

## X-Ray Diffraction

Oriented clays were prepared on ceramic plates and XRD patterns from 4-30 °2θ were obtained after various pretreatments to aid identification of minerals (Brown and Brindley, 1980). Whole samples, silt fractions, kaolin and iron concentrates were investigated by X-ray powder diffraction (XRD). Random powder patterns were obtained using CuKα radiation with a Philips PW-3020 diffractometer equipped with a graphite diffracted beam monochromator. The kaolin and iron concentrates contained 5% NaCl as an internal standard to enable accurate spacing and line broadening measurements. The random powder pattern of kaolin were

obtained over the range of 4-65 °2θ to measure values and to determine the degree of structural order of the kaolins expressed as the HB crystallinity index (Hughes and Brown, 1979). Coherently scattering domain (CSD) size of kaolin along the c-axis direction was calculated from the width at half height of the 001 and 060 reflections using the Scherrer equation (Klug and Alexander, 1974). X-ray diffraction patterns of iron oxide concentrates were recorded from 4-70 °2θ. The spacings of reflections were interpreted to determine Al substitution in goethite (Schwertmann and Carlson, 1994) and hematite (Schwertmann, 1988). Mean coherently diffracting length (MCD, equivalent to CSD) was calculated from the width of 110 reflections of goethite and hematite using the Scherrer formula, after correction for instrumental broadening (Schulze, 1984).

## Transmission Electron Microscopy

A very dilute suspension of the <2 mm size fraction of 6 clay samples and 2 kaolin concentrates was dispersed by ultrasonic treatment. A drop of suspension obtained using a Jeol 2000 FX II electron microscope operated at 80 kV and the image was deposited onto a carbon coated grid and dried at room temperature. Micrographs were obtained using a Jeol 2000 FX II electron microscope operated at 80 kV and an image analysis program (ImageJ 1.34S) was used to measure crystal shape parameters. An X-ray energy dispersive analytical system (EDS) on a JEOL 3000 FEG electron microscope operated at 300 kV was used to analyze 6 representative clay samples and individual kaolin particles in Ti3 and Nb1.

## Results and Discussion

### Soil Characteristics

These Thai upland soils are Oxisols and Ultisols that experience a udic soil moisture regime and have formed on diverse parent materials (Table 1). The soils exhibit a wide range of soil properties depending on their parent materials (Table 2). The Oxisols have formed from basalt and limestone and are very deep soils with the texture of clay or silty clay throughout the profile. Horizonation is not evident since dispersed iron oxides are present throughout the profile resulting in a uniform color.

However, kandic and/or oxic horizons are present. The soils are acidic throughout the profiles with the pH value being 4.2-6.5. The neutral reaction in some topsoil samples may be due to agricultural liming. Values of organic matter, available P, available K, EA and CEC are higher for Oxisols derived from basalt than for those from limestone (Table 2). Crystalline iron oxides as estimated by DCB extraction ( $Fe_d$ ) are the dominant form of iron oxide in these soils and the amounts differ between basaltic (mean=97 g kg<sup>-1</sup>) and limestone-derived Oxisols (mean=69 g kg<sup>-1</sup>).  $Fe_d$  in Oxisols (39-150 g kg<sup>-1</sup>) is almost constant with depth as these soils have quite uniform texture trends. The  $Fe_o$  which indicates the noncrystalline iron oxide (e.g. ferrihydrite) is much higher for the basaltic soils (Ti and Nb series) than for soils formed on limestone (Ak and Ptu).

Ultisols have a pronounced argillic horizon since extensive illuviation has taken place. The texture of these soils is loamy sand to sandy clay loam and is considerably lighter than that of Oxisols. The range of pH for Ultisols is from 3.7-6.4. Ultisols from both granite and sedimentary rock have lower values of organic matter, available P, available K and CEC than do the Oxisols because of the greater sand content of Ultisols.  $Fe_d$  in Ultisols (0.27-30 g kg<sup>-1</sup>) increases with depth as the subsoil contains more clay than does the topsoil. Values of  $Fe_d$  for Ultisols are much smaller than for Oxisols. The  $Fe_o$  content of Ultisols (0.27-4.87 g kg<sup>-1</sup>) is also lower than for the Oxisols. However values of  $Fe_o/Fe_d$  for Ultisols are higher than that of Oxisols indicating that there is a larger proportion of noncrystalline iron oxides in Ultisols which may possibly indicate a lower degree of weathering for these soils (Lair et al., 2009).

**Table 2** Physicochemical properties of Thai upland Oxisols and Ultisols for four parent materials.

Property	Oxisols (mean±SD)		Ultisols (mean±SD)	
	Basalt (n=39)	Limestone (n=21)	Granite (n=30)	Sedimentary rock (n=37)
pH (1:1 H <sub>2</sub> O)	4.8±0.28	5.5±0.27	4.3±0.18	5.0±0.39
pH (1:1 KCl)	4.4±0.22	4.0±0.41	3.6±0.16	3.7±0.30
OM (g kg <sup>-1</sup> )	13±19	5.7±4.7	3.7±3.1	6.1±5.1
Total N (g kg <sup>-1</sup> )	0.62±0.69	0.37±0.24	0.17±0.15	0.24±0.13
Avail. P (mg kg <sup>-1</sup> )	47±27	8.1±28	5.1±8.4	2.6±6.4
Avail. K (mg kg <sup>-1</sup> )	25±22	14±7.8	14±5.7	13±6.3
Extr. Al (cmol kg <sup>-1</sup> )	0.20±0.31	1.0±0.79	1.7±0.41	0.96±0.93
EA (cmol kg <sup>-1</sup> )	26±17	9.5±1.7	3.0±1.6	5.3±3.5
Sum bases (cmol kg <sup>-1</sup> )	2.0±2.2	3.4±1.7	1.3±1.4±	0.7±0.6
CEC (cmol kg <sup>-1</sup> )	13±5.2	8.3±1.5	3.3±1.6	3.3±1.3
ECEC (cmol kg <sup>-1</sup> )	5.8±5.2	4.4±1.6	2.9±1.5	1.7±1.0
BS (%)	11±7.7	26±11	43±39	13±12
Sand (g kg <sup>-1</sup> )	73±55	196±127	505±144	562±149
Silt (g kg <sup>-1</sup> )	231±99	74±43	78±38	123±42
Clay (g kg <sup>-1</sup> )	697±138	730±164	417±138	315±166
SSA (m <sup>2</sup> g <sup>-1</sup> )	75±6.3	37±6.8	16±6.6	12±8.4
$Fe_d$ (g kg <sup>-1</sup> )	97±25	69±14	9.3±8.5	11±8.0
$Al_d$ (g kg <sup>-1</sup> )	21±2.8	6.3±1.2	3.2±2.2	3.6±1.4
$Mn_d$ (g kg <sup>-1</sup> )	2.9±0.83	0.76±0.40	0.010±0.020	0.14±0.14
$Fe_o$ (g kg <sup>-1</sup> )	16±3.1	2.1±0.73	1.5±0.91	1.0±0.63
$Al_o$ (g kg <sup>-1</sup> )	9.7±3.7	8.0±3.4	1.5±0.54	3.1±1.7
$Mn_o$ (g kg <sup>-1</sup> )	2.0±1.0	0.29±0.37	0.018±0.016	0.086±0.12
$Fe_p$ (g kg <sup>-1</sup> )	2.9±4.7	0.17±0.14	0.78±2.1	0.74±1.7
$Al_p$ (g kg <sup>-1</sup> )	5.1±5.6	2.0±0.69	1.5±0.93	2.1±2.3
$Mn_p$ (g kg <sup>-1</sup> )	0.071±0.11	0.10±0.13	0.004±0.002	0.023±0.026
$Fe_o/Fe_d$	0.21±0.28	0.032±0.017	0.39±0.52	0.37±0.75

## Mineralogy of Whole Soils and Silt Fractions

XRD patterns were obtained for representative samples of randomly oriented whole soil and silt fraction. Results are expressed as a semi-quantitative mineralogy (Table 3). The whole soil samples of Oxisols contain much kaolinite with moderate amount of quartz whereas quartz is the dominant mineral and kaolinite is subordinate for Ultisols. Goethite, hematite, maghemite and gibbsite are significant constituents of Ti and Nb Oxisols which are soils derived from basalt. A trace amount of anatase occurs in all soils. The random powder X-ray diffraction patterns of the silt fraction of all these soils give strong reflections of quartz indicating that it is the dominant mineral of the silt fraction. Anatase, zircon and rutile are minor minerals in the silt of all Oxisols and Ultisols. Kaolinite,

maghemite, gibbsite and hematite are present as minor minerals in the silt fraction of Oxisols.

## Mineralogy of Clay Fractions

The clay fractions of these soils contain a large amount of kaolin group minerals with various amounts of minor accessory clay minerals including illite, and hydroxy-Al interlayered vermiculite (HIV) together with quartz, goethite, hematite, maghemite, gibbsite and anatase (Table 3). Iron oxides (goethite and hematite) and HIV occur in moderate amounts in Oxisols and in minor amounts in Ultisols. The dominance of kaolin group minerals and iron oxides in these soils strongly influences the chemical and physical properties of the soils (Schwertmann and Taylor, 1989). Therefore the properties of these minerals have been investigated in detail.

**Table 3** Semi-quantitative mineralogy of whole soil, silt and clay fractions<sup>1/</sup>.

Soil series	Whole soil				Silt fraction				Clay fraction				
	Very much	Much	Moderate	Little	Very much	Much	Moderate	Little	Very much	Much	Moderate	Little	
<i>Oxisols</i>													
Ak1	-	Kao, Qtz	-	Ant	Qtz	-	-	-	Kao, Ant, Rut	Kao	-	Hem	HIV, Qtz, Goe, Ant
Ak2	-	Qtz	Kao	Ant	Qtz	-	-	-	Kao, Goe, Ant, Rut	Kao	-	Hem	HIV, Qtz, Goe
Ptu	Qtz	-	-	Kao, Ant	Qtz	-	-	-	Kao, Ant, Rut, Zr	Kao	-	HIV, Hem	Goe, Ant
Ti1	-	Kao	Qtz, Goe	Gib, Hem, Mh, Ant	-	Qtz	Hem, Mh, Rut, Zr	Kao Gib, Hem	Kao	-	HIV, Hem, Goe	Mh, Gib, Ant	
Ti2	-	Kao	Qtz, Goe	Gib, Hem, Mh, Ant	-	Qtz	Hem, Mh	Kao, Gib	Kao	-	HIV, Hem, Goe	Mh, Gib, Ant	
Ti3	-	Kao	Qtz, Goe	Gib, Hem, Mh, Ant	-	Qtz	Mh	Kao, Gib, Hem, Ant	Kao	-	HIV, Hem, Goe, Mh	Gib, Ant	
Nb1	-	Kao	Qtz, Goe	Gib, Mh, Ant	-	Qtz	Ant	Kao, Gib, Goe, Mh	Kao	-	HIV, Goe	Ill, Qtz, Gib, Mh, Ant	
Nb2	-	Kao	Qtz, Mh	Gib, Goe, Hem, Ant	-	Qtz	Mh	Kao, Gib, Goe, Hem, Ant	Kao	-	HIV, Hem	Ill, Qtz, Goe, Gib, Mh, Ant	
<i>Ultisols</i>													
Kh	Qtz	-	-	Kao, Ant, Goe	Qtz	-	-	-	Kao, An	Kao	-	HIV	Ill, Goe, Hem, Ant
Kc	-	Qtz	Kao	Ant	Qtz	-	-	-	Ant, Rut	Kao	-	-	HIV, Qtz, Goe, Hem, Ant
Fd	Qtz	-	-	Kao, Ant	Qtz	-	An	Zr	Kao	-	Qtz	HIV, Goe, Hem, Ant	
Kbi	Qtz	-	-	Kao, Ant	Qtz	-	-	Kao, Ant, Rut, Zr	Kao	-	Qtz, HIV	Goe, Hem, Ant	
Sd	Qtz	-	-	Kao, Ant	Qtz	-	-	Ant, Zr	Kao	-	HIV	Qtz, Goe, Hem, Ant	
Pk	-	Qtz, Kao	-	Ant	Qtz	-	-	-	Kao	Kao	-	-	HIV, Ill, Qtz, Goe, Ant
Pga	Qtz	-	-	Kao, Ant	Qtz	-	-	-	Ant, Rut	Kao	-	-	HIV, Ill, Qtz, Goe, Hem, Ant
Tim	Qtz	-	-	Kao, Ant	Qtz	-	-	-	Ant, Rut	Kao	-	-	HIV, Ill, Qtz, Goe, Ant
Hp	Qtz	-	-	Kao, Ant	Qtz	-	-	-	Ant, Rut	Kao	-	Qtz	Ill, Ver, Ant

<sup>1/</sup> Very much = > 60%; Much = 20-60%; Moderate = 5-20%; Little = <5%; - = not detected; Qtz = quartz, Kao = kaolin group minerals, HIV = hydroxy-Al interlayered vermiculite, Ill = illite, Ver= vermiculite, Goe = goethite, Hem = hematite, Mh = maghemite, Gib = gibbsite, Ant = anatase, Rut = rutile, Zr = zircon.

## Properties of Kaolin Group Minerals

The kaolin samples contain minor amounts of quartz and gibbsite, particularly for soils derived from basalt. Minor amount of anatase, hydroxy-Al interlayered vermiculite and illite are also present in some kaolin samples.

### Morphology

The shape of kaolin crystals observed by TEM differ substantially between soils (Figure 1). Perfect euhedral hexagonal crystals are common for kaolin derived from granite (e.g. Hp, Pga, Pk and Tim), sedimentary rocks (e.g. Kc and Sd) and limestone (e.g. Ak1) whereas they are rare in basaltic soils. This trend has been observed by other workers (Hughes and Brown, 1979; Hart et al., 2003). There is a wide range of crystal sizes for kaolin in Kbi and Kh soils. The small crystals may have formed directly during pedogenesis whereas the large crystals may have been inherited from the parent sedimentary rock where diagenesis commonly produces large crystals of kaolin (Montes et al., 2002). Alternatively large kaolin crystals may have formed in saprolite that occurs beneath the present soil profile.

Halloysite tubes occurred together with platy crystals in Kh, Kbi and Sd soils and in all basaltic soils. Many studies indicate that basaltic soils in warm and wet climates contain halloysite (Kautz and Ryan, 2003; Zhang et al., 2007; Rasmussen et al., 2010). Halloysite being less ordered than kaolinite may be more susceptible to weathering. In some strongly weathered soils, halloysite is more common than kaolinite but it is less stable and it may be replaced by kaolinite with time (Quantin, 1990; Navarrete et al., 2007).

Histograms of the frequency of values of the shape ratio ( $SR = \text{length}/\text{width}$ ) of platy kaolinite crystals (Figure 2) derived from TEM micrographs indicate that the mean value is considerably greater than one because some kaolinite crystals are elongated. The mean value of shape ratio ranges from 1.26 to 1.47 for Ultisols and from 1.31 to 1.51 for Oxisols. The proportions of lath shaped and equant particles were calculated with a SR value = 2.0 being taken as the boundary between the two shapes. Thus  $SR > 2.0$  identifies a lath and  $SR < 2.0$  identifies an equant crystal. The proportion of lath shaped particle is highest in Nb1 (10%) and

consequently the mean value of shape ratio for this soil is the highest (Table 4). Laths are a common morphological feature of kaolin pseudomorphs after mica (Pei Yuan Chen et al., 2004) and this soil although primarily developed over basalt contains minor amount of a micaceous mineral.

Coherently scattering domain (CSD<sub>001</sub>) sizes of kaolin crystals derived from the width at half height (WHH) of XRD reflections and calculated using the Scherrer equation indicate that the average size of soil kaolin crystals along the c-axis ranges from 10.1 to 20.4 nm for Oxisols and from 14.0 to 41 nm for Ultisols. The kaolins derived from basalt have the smallest crystal size (mean=11.8 nm) whereas kaolin in all other soils has a similar mean value of crystal size after omitting outlier data for Kbi soil (i.e. granite=16.9 nm, limestone and other clastic sedimentary rock=18.5 nm).

### Chemical composition

The chemical composition of kaolin bulk samples determined by XRF shows that considerable titanium (Ti) is present in all kaolin samples and amounts of Ti are higher in kaolin from Oxisols (mean 33 g kg<sup>-1</sup>) than from Ultisols (mean=14 g kg<sup>-1</sup>) (Table 4). Concentrations of Ti are particularly high for kaolin samples from basaltic soils. Significant amount of potassium are present in all kaolin samples except for Ak1 profile where K was not detected by XRF. The K<sub>2</sub>O in kaolin is less than 10 g kg<sup>-1</sup> for all soils except for Hp Ultisol which has the highest K<sub>2</sub>O (16 g kg<sup>-1</sup>) and Nb1 and Nb2 kaolins contain more K than do other Oxisols. These kaolin samples contain small amounts of illite. Kaolin crystals in tropical soils may contain a minor amount of interlayer K in rare illite layers but this proposition has yet to be confirmed as a common occurrence (Melo et al., 2001).

A striking feature of the chemical composition of soil kaolin compared with ideal kaolinite is the presence of considerable amounts of Fe despite free iron oxides having been removed by the DCB treatment. The Fe<sub>2</sub>O<sub>3</sub> content in the deferrated kaolin ranges from 1.0 to 28 g kg<sup>-1</sup>. The mean Fe<sub>2</sub>O<sub>3</sub> content of kaolin in Oxisols (mean=18 g kg<sup>-1</sup>) is the same as for Ultisols (mean=17 g kg<sup>-1</sup>) indicating that the substitution of Fe in kaolin does not simply depend on the Fe content of the parent

**Table 4** Some properties of purified kaolin and iron oxides in Thai Oxisols and Ultisols.

Soil series/ horizon	Depth (cm)	Kaolin										Goethite		Hematite				
		TiO <sub>2</sub> (-----g kg <sup>-1</sup> -----)	Fe <sub>2</sub> O <sub>3</sub>	K <sub>2</sub> O	CSD <sub>001</sub>	CSD <sub>060</sub>	HB index	SSA (m <sup>2</sup> g <sup>-1</sup> )	CEC (cmol kg <sup>-1</sup> )	Length (-----nm-----)	Width (-----nm-----)	Lath (-----%-----)	Equant (%)	Tube (nm)	Mole Al	MCD <sub>110</sub>	Mole Al	MCD <sub>110</sub>
<i>Oxisols</i>																		
Ak1/ Bt02	42-70	9.2	10.3	nd	17.3	28.7	4.7	22	7.0	101	77	4	96	nd	15	22	11	29
Ak2/ Bt03	60-90	26.7	9.8	0.47	17.8	32.4	5.2	22	6.4	110	82	7	93	nd	17	28	9	25
Ptu/ Bt02	46-75	13.8	14.5	1.2	20.4	21.7	5.6	26	7.6	78	60	6	94	nd	15	30	10	29
Ti1/ Bt01	27-52	45.9	27.0	0.45	10.4	16.4	5.3	48	18	69	52	5	90	5	19	12	15	16
Ti2/ Bt02	40-70	43.7	19.9	0.41	11.5	18.5	4.5	64	19	99	74	9	82	9	17	12	10	15
Ti3/ Bt01	67-100	45.4	27.5	0.65	10.1	7.9	7.5	65	19	99	73	2	79	9	23	9	7	15
Nb1/ Bt3	65-95	46.1	18.3	4.9	13.4	12.1	7.1	48	15	84	57	10	79	10	21	11	nd	nd
Nb2/ Bt3	50-80	35.5	15.2	3.2	11.5	11.2	9.5	51	19	91	61	6	87	7	10	17	6	13
Mean	-	33.3	17.8	1.4	14.1	18.9	6.2	43	14	91	67	-	-	-	17	18	9.7*	20*
<i>Ultisols</i>																		
Kh/ Bt2	50-80	11.3	11.8	8.2	24.2	13.6	10.4	31	16	109	77	7	75	8	14	18	12	18
Kc/ Bt2	32-52	13.8	22.4	0.27	17.3	18.1	6.1	41	6.5	106	79	2	98	nd	18	8	6	19
Fd/ Bt4	78-103	15.0	14.5	0.81	17.1	28.3	5.0	23	14	110	89	3	97	nd	16	23	7	33
Kbi/ Bt3	65-93	16.5	10.6	1.3	40.6	31.8	9.2	17	9.2	219	152	4	91	5	16	26	9	44
Sd/ Bt3	81-110	17.5	16.7	1.7	15.2	24.6	5.7	28	7.4	131	106	3	96	1	13	34	10	33
Pk/ Bt3	60-80	4.7	11.6	1.7	17.9	18.2	10.7	40	6.0	150	105	7	93	nd	19	17	7	15
Pga/ Bt3	78-110	10.7	21.4	3.3	19.1	20.5	9.2	34	12	128	89	3	97	nd	nd	nd	nd	nd
Tim/ Bt3	74-104	15.9	19.8	3.6	16.5	16.8	9.0	36	9.0	124	86	5	95	nd	11	11	6	19
Hp/ Bt1	35-65	18.4	19.7	16.4	14.0	12.4	8.5	34	8.0	115	87	2	98	nd	nd	nd	nd	nd
Mean	-	13.7	16.5	4.1	19.7	21.3	7.9	32	9.0	132	97	-	-	-	13*	17*	7.5*	27*

\* The calculated mean excludes not detectable (nd) goethite/hematite.

rock or the total Fe content of the soils, both of which are largest for the basaltic soils. Thus Fe<sub>2</sub>O<sub>3</sub> values of 15 to 18 g kg<sup>-1</sup> in kaolin from Nb1 and Nb2, (basalt-derived soils), were lower than the mean value ( $\approx$  20 g kg<sup>-1</sup>) for kaolin from granitic soil profiles (Hp, Pga and Tim).

Several workers have demonstrated a significant negative relationship between the crystal size of kaolin and Fe<sub>2</sub>O<sub>3</sub> concentration (Hart et al., 2003; Hughes et al., 2009). This study also observed significant negative relationships between kaolin crystal size CSD<sub>001</sub> and Fe content for kaolin in Oxisols. ( $R^2=0.56^{***}$ ,  $p=<0.001$ ) and Ultisols ( $R^2=0.29^{**}$ ,  $p=<0.01$ ). However, no relationship

exists between CSD<sub>060</sub> and Fe content for Ultisols (Figure 3).

Kaolin in these soils is highly disordered with a mean HB index value for Oxisols of 6.2 and for Ultisols of 8.2 indicating a lack of structural order and these HB values are much less than HB index values for reference mineral kaolinite which range from 38 to 83 (Hughes and Brown, 1979; Singh and Gilkes, 1992a). Although some studies have shown negative relationships between the Fe content of soil kaolin and crystallinity (Hart et al., 2002; Singh and Gilkes, 1992a) other workers have not found this relationship (Trakoonyingcharoen et al., 2006a) as is for the case for the present study (Figure 3).

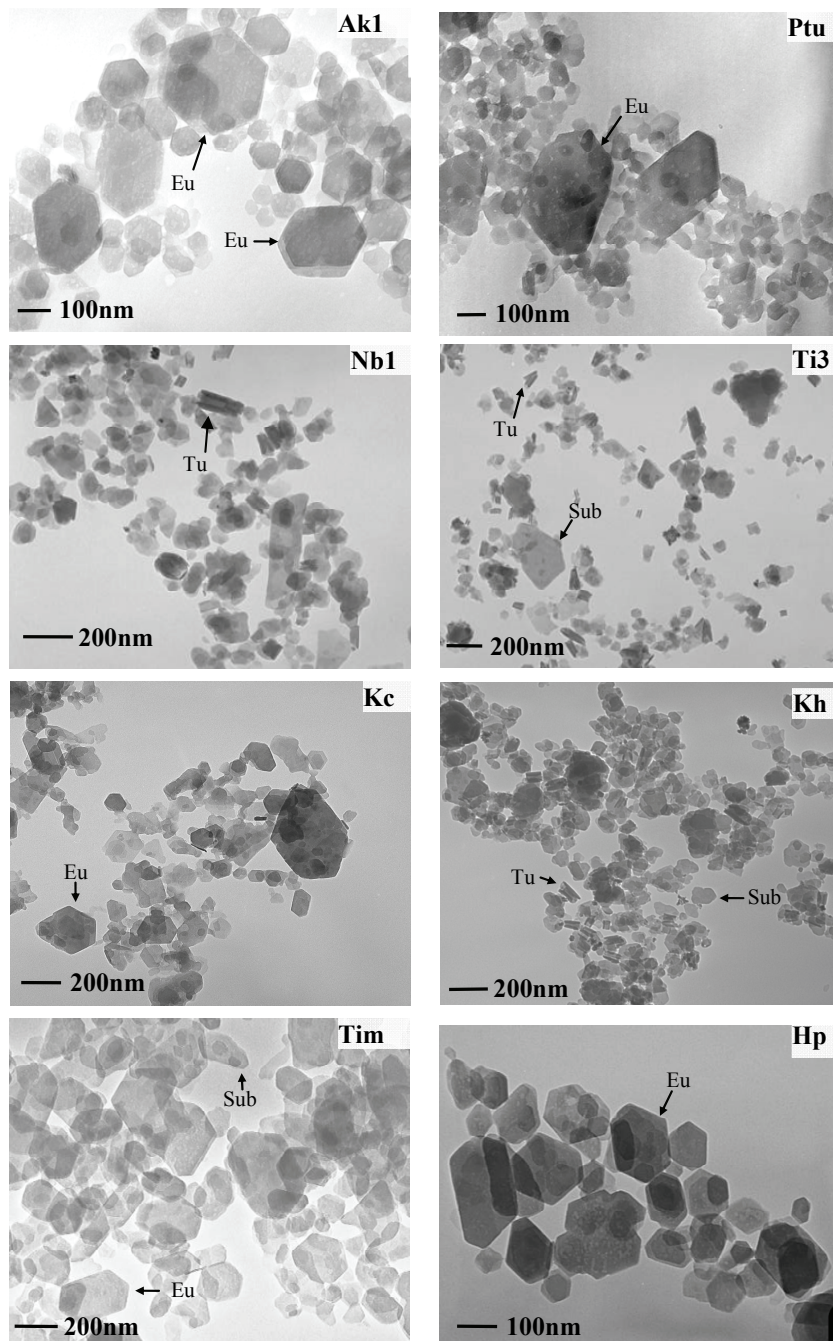


**Figure 1** Transmission electron microscope (TEM) micrographs of deferrated kaolins from soils derived from various parent materials showing the wide variation of crystal morphology and size. Sub = subhedral faces, Eu = euhedral faces and Tu = tubes.

#### **Specific Surface Area (SSA) and Cation Exchange Capacity (CEC)**

The specific surface area of these kaolins has a wide range ( $17\text{-}65 \text{ m}^2 \text{ g}^{-1}$ ). The highest surface area is for Ti3 kaolin which is consistent with its very small crystal size. The low SSA for kaolin in profile Kbi relates to the large crystal size of kaolin in this soil. The SSA of kaolin in Oxisols has a weak positive

relationship with Fe content but this relationship does not exist for Ultisols (Figure 3). The lack of clear relationships may reflect the quite small range of Fe concentrations in these kaolins. The cation exchange capacity of the kaolins ranges from  $7\text{-}19 \text{ cmol kg}^{-1}$ . The CEC is closely related to crystal size of kaolin as there is a general trend for CEC to increase with decreasing crystal size and increasing

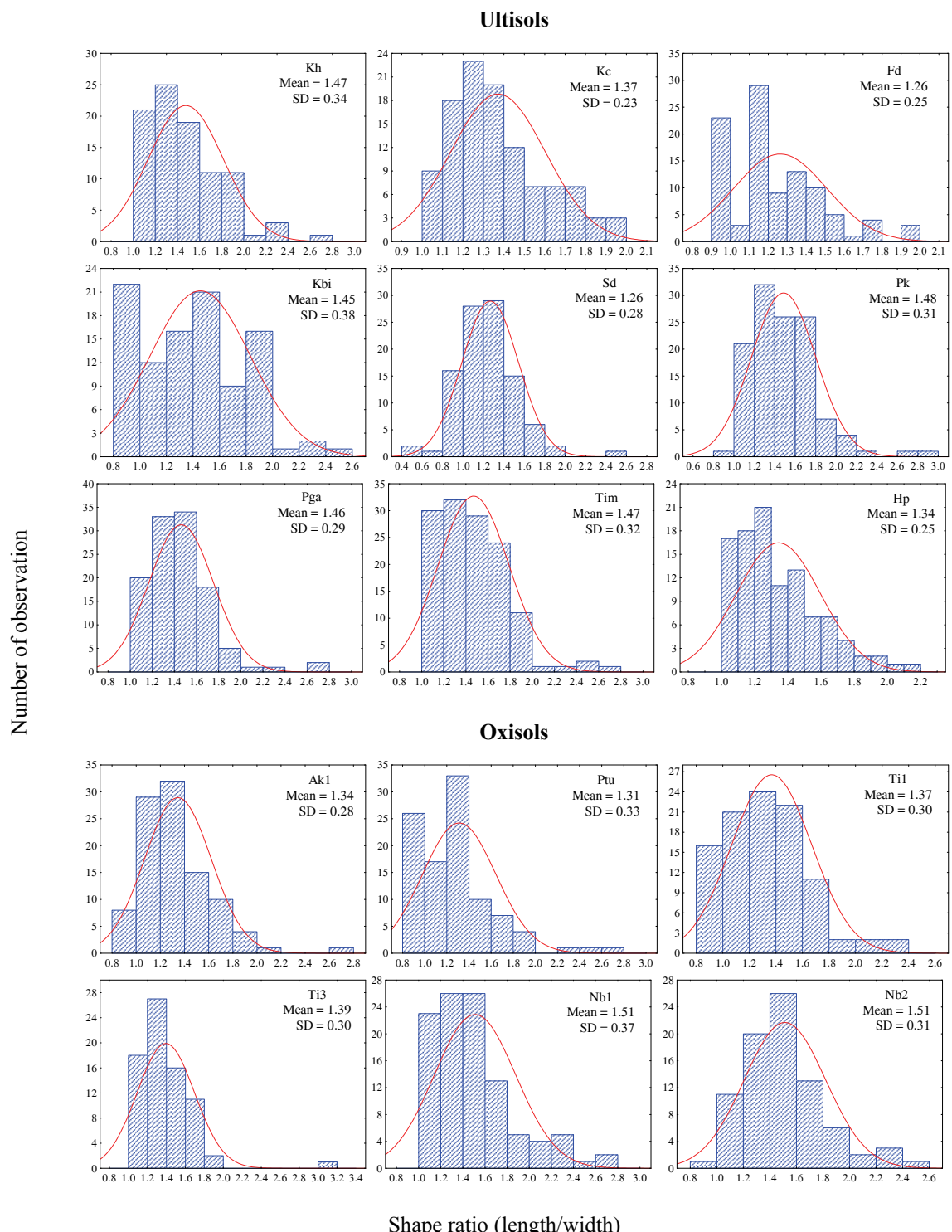


**Figure 2** Histograms of the frequency of occurrence of kaolin crystals with various values of shape ratio (length/width) determined by TEM for soil deferrated kaolins from representative Oxisols and Ultisols developed on diverse parent materials.

SSA (Figure 4). Halloysite tubes contribute to the higher SSA and CEC of kaolin concentrates from Oxisols relative to that from Ultisols as halloysite

exhibits larger surface area (Bigham et al., 2002) and cation exchange capacity than kaolinite (Delvaux et al., 1990).

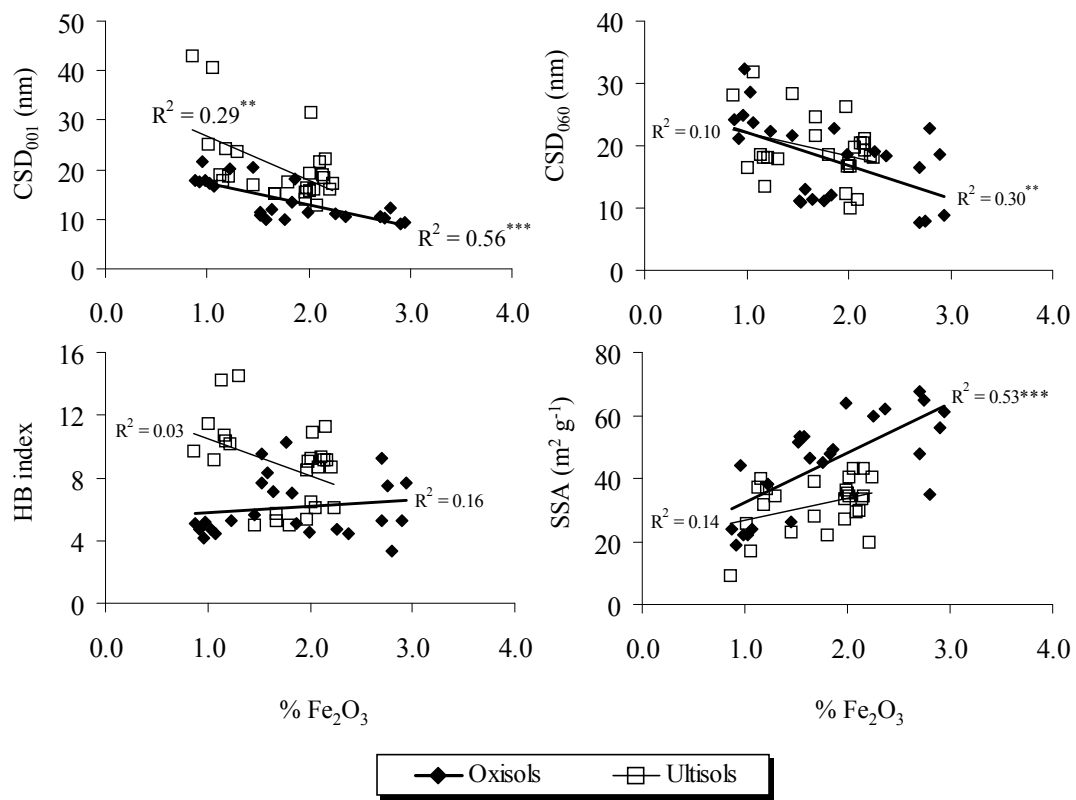


**Figure 3** Relationships of CSD<sub>001</sub>, CSD<sub>006</sub>, crystallinity index and SSA with %Fe<sub>2</sub>O<sub>3</sub> for deferrated soil kaolins. \*P < 0.05; \*\*P < 0.01; \*\*\*P < 0.001.

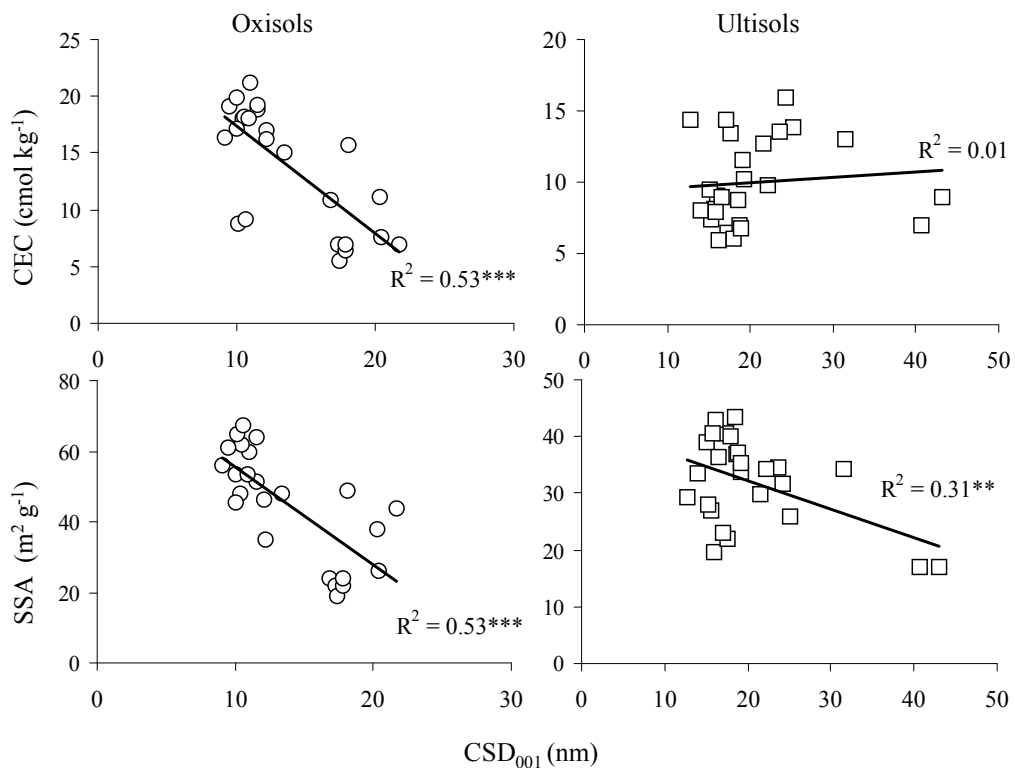


**Figure 4** Relationships between SSA, CEC and CSD<sub>001</sub> for soil kaolins. \*\*P < 0.01; \*\*\*P < 0.001.

## Properties of Iron Oxides

### *Al substitution in goethite and hematite*

The degree of Al substitution in iron oxides in soils reflects the environment in which they formed and in particular the relative activities of Al and Fe in soil solution (Schwertmann and Kämpf, 1985; Schwertmann, 1988). Iron oxide in the clay fractions from 15 representative samples from each profile were concentrated by dissolving kaolin in 5M NaOH. Hp and Pga soils were not investigated as they contain little or no iron oxides in the clay fraction (Table 3). Measurement of Al substitution based on precise values of XRD spacing indicates 10-23 mole% Al in goethite and 6-15 mole% Al in hematite (Table 4). The values of mole% Al substitution in both goethite and hematite in Oxisols are slightly higher than that in Ultisols. Goethite in profile Ti3 has the highest levels of Al substitution. Basaltic soils have high Al substitution in goethite and hematite and these soils contain gibbsite, which may indicate that the pedogenic environment promotes desilication of primary minerals and release of abundant free Al which substitutes for Fe in iron oxides (Motta and Kämpf, 1992). There is no relationship between mole% Al substitution in goethite and hematite for these soils (Figure 5) in contrast with observations of many workers (Siradz, 2000; Prasetyo and Gilkes, 1994; Schwertmann and Kämpf, 1985) who showed that a strong positive relationship existed for some tropical soils. The poor statistical strength of this relationship in the present research is probably partly due to the small range of Al substitution values for both iron oxides.

As postulated by Schwertmann (1988), a small level of Al substitution may stabilize the structure of iron oxide minerals by releasing structural strain, so that a small amount of Al is readily accepted by the iron oxide structure. Increasing substitution of Al may increase structural strain, slow the rate of crystal growth and reduce crystal size. However this study shows no relationship between mole% Al substitution and crystal size (MCD) for both hematite and goethite (Figure 5). The MCD of goethite in Oxisols follows the sequence basalt< granite< clastic sedimentary rocks = limestone and a similar trend occurs for hematite.

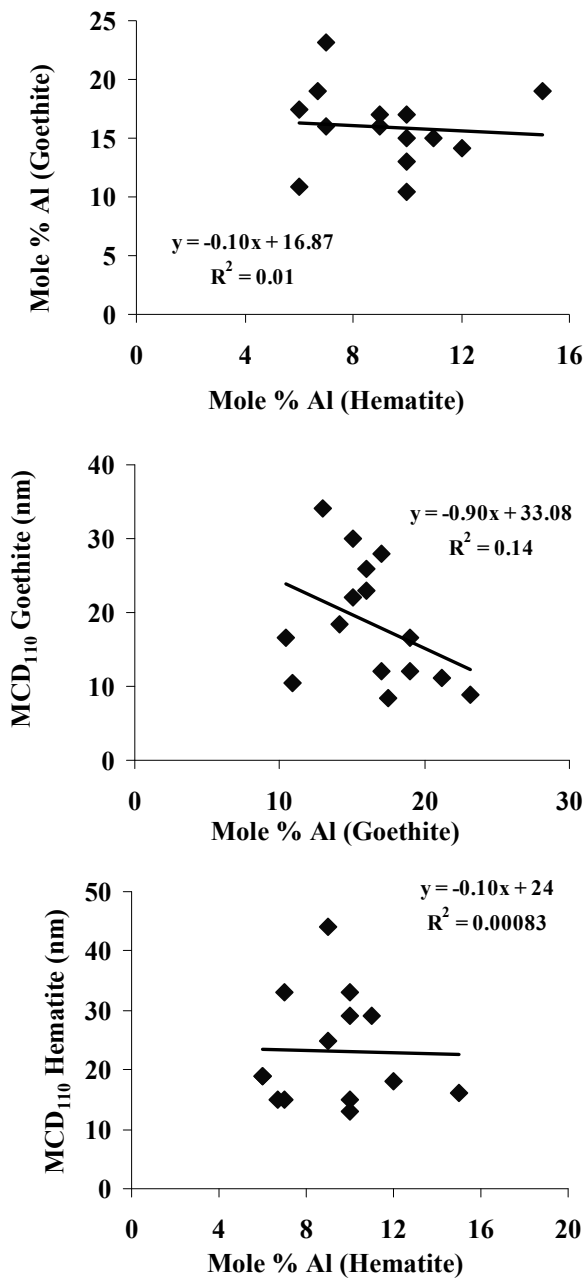


**Figure 5** Bivariate plots showing the absence of relationships between mole% Al substitution in goethite and hematite and for MCD<sub>110</sub> of goethite and hematite versus mole% Al for iron oxide concentrates.

### *Amorphous Fe oxides*

Amorphous Fe oxides ( $\text{Fe}_\text{o}$ ) are considered unstable under most soil conditions and significant amounts are expected to be present only during initial stage of soil formation. However, the mature highly weathered soils derived from basalt (Ti and

Nb) contain much amorphous Fe, probably as ferrihydrite, possibly due to the presence of abundant dissolved silica and organic matter impeding formation of crystalline Fe oxides (Cornell and Schwertmann, 2003). The high annual rainfall of the region where the basaltic soils profiles occur ( $\sim 3300$  to  $3500$  mm of annual rainfall) may result in the rate of dissolution of the parent rock exceeding the rate of formation of kaolin and crystalline iron oxide resulting in the presence of non-crystalline forms of Fe and Al in the soil (Arieh, 1966). Higher values of  $Fe_o$  may also be due to the greater solubility in oxalate of crystalline iron oxides in these basaltic soils which have much smaller iron oxide crystals than are present in the other soils (Trakoonyingcharoen et al., 2006b). With increasing soil age, Fe compounds accumulate and noncrystalline forms including ferrihydrite transform into more stable crystalline minerals particularly goethite and hematite. Ti and Nb clays contain relatively higher amounts of goethite in the clay fraction indicating that ferrihydrite may transform to goethite rather than to hematite.

Sesquioxide minerals have high SSA and may contribute to the higher SSA of Oxisols relative to Ultisols. There are significant positive relationships between SSA and both  $Fe_d+Al_d$  and  $Fe_o+Al_o$  of Oxisols whereas there is no relationship for Ultisols (Figure 6). The  $R^2$  values for the linear relationships between SSA and iron content ( $Fe_d$  and  $Fe_o$ ) are very high but the distribution of data is bimodal so the statistical relationship is an unreliable indicator of a continuous relationship. Including the extractable Al (i.e.  $Fe_o+Al_o$ ,  $Fe_d+Al_d$ ) provides statistically robust relationships. Compared to crystalline iron oxides such as goethite and hematite, amorphous Fe and Al oxides have larger surface area (Borggaard, 1990) as indicated by these relationships.

### TEM-EDS analysis

The composition of single clay-size, complex particles from the nondeferrated clay fraction of several samples as determined by TEM- EDS (energy dispersive spectrometry) analysis (Figure 7) have been expressed as normalized percentages of  $SiO_2$ ,  $Al_2O_3$  and  $Fe_2O_3$  on a water-free basis and are plotted in a triangular graph (Figure 7b). Analyses of ideal kaolin crystals should be located

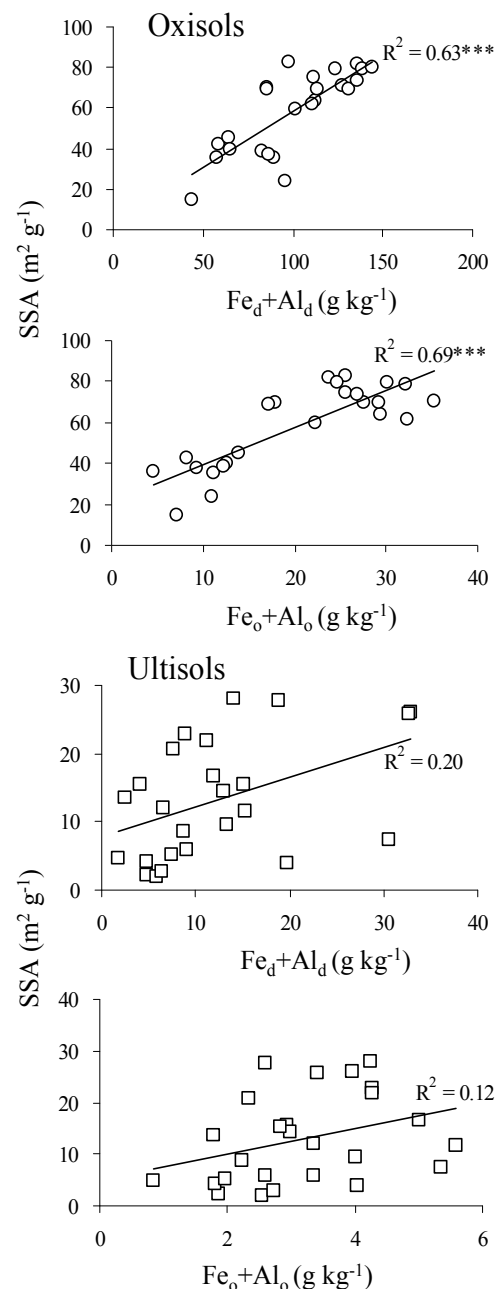


**Figure 6** Relationships between SSA of soil samples and Fe plus Al extracted from soil by dithionite-citrate-bicarbonate and ammonium oxalate solutions for Oxisols and Ultisols. \*\*\* $P < 0.001$ .

on the horizontal axis of the triangular graph at 55%  $SiO_2$  and 45%  $Al_2O_3$ . The small quantities of structural iron present in kaolin crystals will result in analysis being slightly displaced from this point towards the  $Fe_2O_3$  apex as is seen in Figure 7c for DCB treated clay. The nondeferrated clay particles include very small particles of iron oxides attached to kaolin crystals (samples Nb1 and Ti3) and this

iron is included in the analyzed volume (Figure 7a). Consequently the analyses of particles plotted in Figure 7b are displaced towards the  $\text{Fe}_2\text{O}_3$  apex along what is defined as the kaolin line. However the analyses for the particularly Fe rich Nb1 and Ti3 kaolins (i.e. for basaltic soils) actually fall on another line which is displaced from the kaolin line towards the  $\text{Al}_2\text{O}_3$  apex and the amount of displacement (excess % $\text{Al}_2\text{O}_3$ ) increases with  $\text{Fe}_2\text{O}_3$  concentration. This displacement is due to the iron oxides particle attached to kaolin crystals being Al-substituted. The degree of Al substitution in goethite in Nb1 and Ti3 clays was estimated by XRD measurements to be about 21% mole (Table 4), the corresponding displaced line is shown in Figure 7b. After removal of iron oxides by DCB treatment from Nb1 and Ti3, the low or nil value of  $\text{Fe}_2\text{O}_3$  (0-1.6 %) in kaolin crystals (Figure 7c) confirms that there is little Fe substitution in kaolin although these soils are Fe-rich and derived from high Fe basalt. The Si/Al ratio for some particles is higher than that for ideal kaolin, this is partly due to Fe substitution for Al but may also be a consequence of damage to particles in the TEM beam which causes preferential Al loss, especially for small and thin kaolin crystals (Ma and Eggleton, 1999).

### Cluster Analysis of Clay Properties

Properties of the clay fraction including properties of kaolin and iron oxides and the SSA and CEC of three fractions (kaolins, clay sample and whole soil samples) for 17 representative soil samples were subjected to cluster analysis and the results are presented as dendograms (Figure 8).

The dendrogram for 27 properties identifies 3 discrete groups of properties (Figure 8a). Cluster 1 consists of variables describing the shape and size of kaolin crystals, cluster 2 consists of the specific surface area of soil, kaolin and clay and cluster 3 consists of various, diverse mineralogical and chemical properties. Cluster 1 is related to cluster 2 in that the size of kaolin crystals has a strong influence on the specific surface area of soil and clay. The amount of illite in the clay is strongly related to the concentration of  $\text{K}_2\text{O}$  in the kaolin. The concentration of  $\text{TiO}_2$  and  $\text{Fe}_2\text{O}_3$  in kaolin are related to the percentage of hematite in the clay fraction. Lath shape which is common morphological feature

of kaolin pseudomorphs after mica is closely related to HIV content. HIV in these soils may be an intermediate step in mica weathering to kaolinite (Cho and Komarneni, 2007). Both HIV and lath shape kaolin are features of Oxisols rather than of Ultisols for these Thai soils.

The cluster for the 17 soil samples (Figure 8b) was produced using 27 variables as shown in Figure 8a. The outlier soil Kbi contains particularly large kaolinite crystals that may have been inherited from the parent material (Table 4). The cluster analyses show a clear distinction between the basaltic soils (all in cluster 1) and the other soils (all except Kbi in cluster 2). The cluster of basaltic soils is characterized by small crystals of both kaolin and iron oxides, and high SSA values for soil, kaolin and clay. Granitic soils clustered together with soils on limestone and other clastic sedimentary rocks.

### Geochemistry of the Clay Fraction

All soil clays contain much Al, Si and Fe with minor amounts of Ti and Mn (Table 5). For soils formed from basalt, the Fe and Ti concentrations in the clay are larger than for other soil clays reflecting the influence of Fe, Ti-rich basalt which contains abundant ferromagnesian minerals and ilmenite. The clay of basaltic soils has more Al than Si whereas the other clays have less Al than Si. The higher proportion of Al in clay of basaltic Oxisols is partly due to desilication under a humid tropical climate with free drainage conditions (Schaefer et al., 2008) causing formation of gibbsite from kaolinite (Muggler et al., 2007). Consequently significant amounts of gibbsite occur in the clay fraction of the Ti and Nb soils. Calcium, Mg and Mn are also present in relatively high concentrations in the clay from basaltic rock as compared to other soil clays. The differences in concentrations of elements in the clay partly reflect the presence of primary minerals inherited from the parent rock (Thanachit et al., 2006). The K concentration in the clay of Ultisols is higher than for Oxisols which is consistent with the presence of illite in some clay fractions (Table 3). Both P and S are much more abundant in the clay from basaltic soils. Both elements occur in soils as oxyanions that are adsorbed by the abundant sesquioxide minerals in these clays so that their greater abundance does not correspond to a greater abundance of these elements in parent rocks.

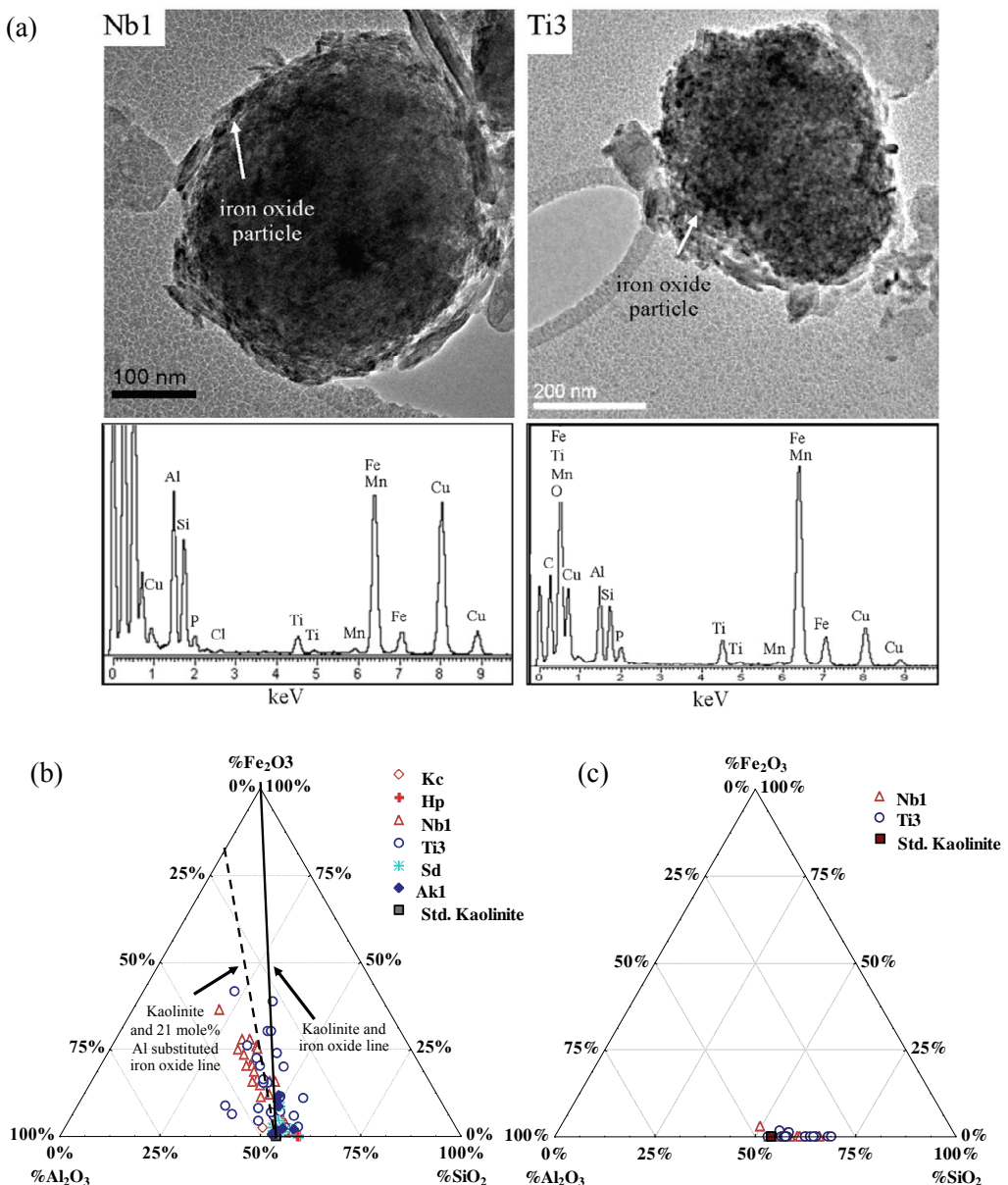


**Figure 7** (a) Micrographs and X-ray spectra from clay particles from Nb1 and Ti3 (not deferrated) showing abundant small (about 10 nm) particles of iron oxides attached to complex aggregated kaolin particle, (b) Triangular graph of elements ( $\text{SiO}_2$ ,  $\text{Al}_2\text{O}_3$ , and  $\text{Fe}_2\text{O}_3$ , normalized composition) from TEM-EDS analyses of clay particles for 6 representative clay samples that had not been deferrated, (c) Triangular graph for deferrated kaolin particles from soils Nb1 and Ti3.

Clay minerals and iron oxides are effective sinks for many trace elements in soils (Singh and Gilkes, 1992b; Becquer et al., 2006) resulting in greater concentrations of trace elements in Oxisols than in Ultisols. The clay fraction of basaltic soils contains significantly higher amounts of Ba, Be, Bi, Ce, Co, Cr, Cu, Ga, La, Nd, Ni, Sc, Sr and Zn. Clays from limestone derived soils contain higher concentrations of As, Pb, V and Zr whereas clays from granitic soils contain higher concentrations of Rb and Th (Table 5).

Principal component analysis of the elementals and mineralogical analyses of the clay fraction was used to identify elements of similar geochemical behavior and also to group clay samples on the basis of their geochemical and clay mineralogical properties. Two factors explain 62.6% of the variation in the data (Figure 9a). The elements and clay mineralogy can be allocated to four main groups of similar geochemical behavior, with some variables not belonging to any group. Group 1 is composed of many major and minor elements (Fe,

Ti, Mg, Mn, Ba, Be, Bi, Ce, Co, Cr, Cu, Ga, La, Nd, Ni, Sc, Sr, Zn) together with amounts of maghemite and goethite in the clay fraction. These variables have large values for clays in basaltic soil (Figure 9b). Many metals are associated with Fe because the metals can substitute for Fe in oxide structures (Kabata-Pendias and Pendias, 2001). Both P and S are quite closely associated with Group 1 elements as they may be adsorbed on sesquioxides as oxyanions (Fontes and Weed, 1996; Wisawapipat et al., 2009).

Group 2 consists of As, Pb, V, Zr, percentage of hematite and HIV. These properties are related to soil clays derived from limestone and also Kbi soil

formed on clastic sedimentary rocks. The concentration of As and Pb is quite high in this soil group (Table 5). Zirconium is classed as residual element in soils and commonly occurs in zircon which is highly resistant to weathering (Cornu et al., 1999; Stiles et al., 2003). Vanadium is frequently found to be associated with Fe oxides and can substitute for Fe in iron oxide minerals (Singh and Gilkes, 1992b; Schwertmann and Pfaff 1996). In the present work, V is most related to hematite. Group 3 composes of K, Rb and illite content and relates to clay samples from granitic soils and Kh soil which was derived from sandstone (Figure 9b). Soil clays from sedimentary rocks

**Table 5** Range and average concentrations (mean±SD) of elements in the clay fraction for upland Oxisols derived from basalt and limestone and upland Ultisols derived from sedimentary rock and granite.

Element	Oxisols						Ultisols					
	Basalt (n=15)			Limestone (n=9)			Sedimentary rocks (n=15)			Granite (n=11)		
	min	max	mean±SD	min	max	mean±SD	min	max	mean±SD	min	max	mean±SD
(g kg <sup>-1</sup> )												
Al	128	173	148±13	152	181	169±10	141	202	172±18	159	195	186±11
Si	122	147	133±7.2	154	188	177±10	171	217	197±13	177	212	202±10
Ti	20	31	23±3.1	4.0	11	6.9±2.0	5.3	11	7.7±1.9	2.3	9.2	5.3±2.2
Fe	107	169	135±21	53	107	82±22	21	92	50±22	14	40	29±11
Mn	1.2	3.3	2.4±0.63	0.31	2.0	0.85±0.61	0.1	1.0	0.37±0.23	0.08	0.15	0.11±0.025
Ca	0.32	2.6	0.92±0.53	0.14	2.3	0.76±0.61	0.11	1.5	0.56±0.38	0.24	0.81	0.48±0.18
K	0.40	2.7	1.4±0.86	0.51	1.1	0.70±0.19	0.24	6.0	2.3±2.1	1.4	6.4	3.4±1.9
Mg	1.6	2.5	2.1±0.22	1.4	2.4	1.8±0.44	0.26	2.3	1.5±0.53	0.84	1.8	1.2±0.32
P	4.6	18	8.2±3.3	0.14	43	5.0±14	0.083	40	4.2±11	nd	41	6.6±14
(mg kg <sup>-1</sup> )												
S	4.2	329	111±96	10	116	41±34	14	508	74±124	7.6	311	67±99
As	nd	3.2	0.5±2.0	21	221	100±81	1.7	84	24±24	1.7	23	8.3±7.5
Ba	329	792	515±154	10	37	19±8.8	12	69	31±18	8	47	30±15
Be	0.73	2.6	1.5±0.69	0.31	1.2	0.61±0.32	0.15	0.41	0.25±0.08	0.13	0.28	0.19±0.040
Bi	6.7	22	13±4.2	2.4	4.3	3.2±0.7	0.61	3.9	1.9±0.92	0.59	3.7	1.7±1.1
Ce	115	174	148±17	30	100	67±25	13	123	54±34	1.7	66	28±23
Co	19	49	36±11	4.8	35.4	12±9.5	3.4	20	8.9±5.2	1.2	2.8	1.9±0.61
Cr	89	192	124±31	55	157	98±40	43	115	73±24	15	60	36±14
Cu	47	75	58±9.6	11	27	19±5.0	12	34	22±7.8	7.7	20	14±4.2
Ga	25	63	44±8.8	24	32.9	28±3.2	14	47	24±7.8	21	58	35±14
La	56	80	69±7.1	12	36	23±8.3	7.0	29	21±7.0	1.1	34	16±11
Mo	1.5	3.9	2.2±0.67	2.2	3.6	2.8±0.48	0.6	8.2	3.1±2.2	0.37	2.1	1.2±0.65
Nd	47	70	59±6.6	10	33	20±7.1	6.9	28	17±6.7	0.72	19	9.5±7.2
Ni	118	283	189±57	19	54	31±13	7.6	32	17±7.2	2.3	9.3	6.3±2.5
Pb	8.2	14	11±1.7	19	51	33±9.8	2.6	38	22±12	4.1	47	17±13
Rb	10	42	22±10	2.8	17	8.0±5.2	2.0	101	37±36	13	72	40±20
Sc	20	30	25±2.6	13	18	15±2.3	3.8	24	14±6.0	1.9	12	7.2±3.6
Sr	244	437	322±56	3	5.9	4.1±1.1	1.9	22	9.7±6.6	2	9.7	6.0±2.7
Th	11	17	14±1.9	18	26	21±2.4	5.7	29	18±8.5	18	70	33±18
V	108	214	155±27	185	299	233±39	34	281	113±69	11	70	33±22
Zn	70	150	105±23	25	90	51±18	20	104	51±31	15	132	40±33
Zr	1.2	6.6	3.0±1.5	5.4	6.8	5.9±0.50	0.82	9.6	4.0±2.4	0.12	3.1	1.7±1.1

nd= not detected

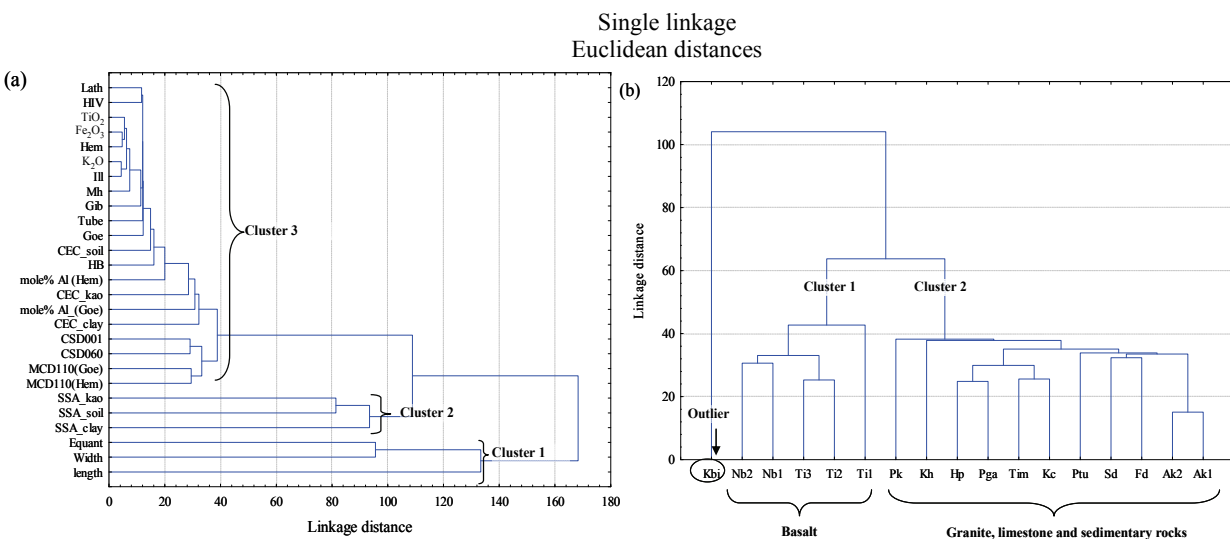


**Figure 8** (a) Cluster analysis for properties of whole soils (CEC and SSA), clay before DCB treatment (mineralogy, CEC and SSA), deferrated clay (crystal shape and size, major elements, CEC and SSA) and iron oxides concentrate (crystal size and %Al substitution) for 17 soils. (b) Cluster analysis for the soils samples using the 27 variables shown in (a).

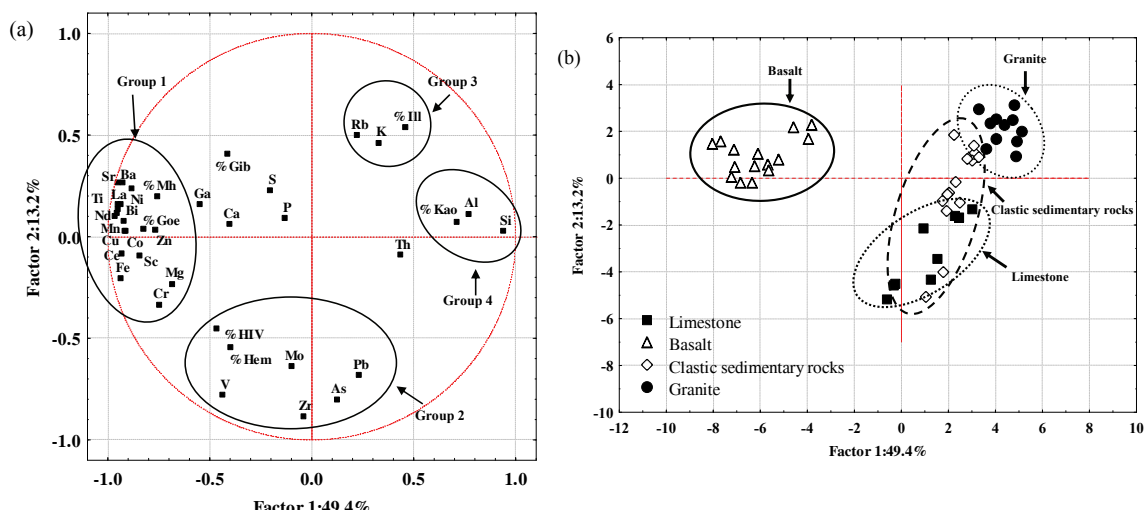


**Figure 9** Factor analysis for mineral and element analyses of the clay fraction of Oxisols and Ultisols developed on diverse parent materials: (a) distribution of mineral analyses and elements; (b) distribution of soils.

show a broad distribution in the opposite quadrant to basaltic soils (Figure 9b). Group 4 of properties contains %kaolin together with the abundances of Al and Si which are the major constituents of kaolin. It is the dilution of the kaolin content of the clay by abundant iron oxides for basaltic soils that separates basaltic soils from all other soils in Figure 9b.

## Conclusions

Analyses on properties and geochemistry of these Oxisols and Ultisols reveal a classic example of lithosequence under tropical monsoonal climate. Under similar topographic condition, natural vegetation and land uses, parent materials show a dominant influence on the mineralogical and chemical

properties of these soils. Though the clay mineralogy of all soils is similar in being dominated by kaolin group minerals and sesquioxides, the properties of these minerals are different. Oxisols derived from basalt contain kaolin group minerals and iron oxides of smaller crystal size and lower crystallinity and with a higher proportion of amorphous material than do soils on other parent materials. Due to their higher content of iron oxides and high clay content, Oxisols derived from basalt have relatively higher contents of most elements. Exceptions are K and Rb which are most abundant in clays from granitic soils. This information on the nature of secondary minerals and the concentrations and associations of elements will be useful for soil fertility management.

### Acknowledgments

This research was supported by the Royal Golden Jubilee Ph.D. Program of The Thailand Research Fund. The authors are grateful to staff of School of Earth and Environment and the Australian Microscopy and Microanalysis Research Facility at the Centre for Microscopy, Characterisation & Analysis, The University of Western Australia for their kind assistance.

### References

- Arieh, S. 1966. The mineralogy of the clay fraction from basaltic soils in the Galilee, Israel. *Eur. J. Soil Sci.* 17: 136-147.
- Aylmore, L.A.G., I.D. Sills and J.P. Quirk. 1970. Surface area of homoionic illite and montmorillonite clay minerals as measured by the sorption of nitrogen and carbon dioxide. *Clays Clay Miner.* 18: 91-96.
- Becquer, T., C. Quantin, S. Rotte-Capet, J. Ghanbaja, C. Mustin and A.J. Herbillon. 2006. Sources of trace metals in Ferralsols in New Caledonia. *Eur. J. Soil Sci.* 57: 200-213.
- Bigham, J.M., R.W. Fitzpatrick and D.G. Schulze. 2002. Iron oxides, pp. 323-366. In: J.B. Dixon and D.G. Schulze, eds., *Soil Mineralogy with Environmental Applications*. SSSA, Madison, Wisconsin.
- Borggaard, O.K. 1990. Dissolution and Adsorption Properties of Soil Iron Oxides. Chemistry Department, Royal Veterinary and Agricultural University, Denmark.
- Brown, G. and G.W. Brindley. 1980. Crystal Structures of Clay Minerals and Their X-ray Identification. Mineralogical Society Monograph No. 5. Mineralogical Society, London.
- Cho, Y. and S. Komarneni. 2007. Synthesis of kaolinite from micas and K-depleted micas. *Clays Clay Miner.* 55: 565-571.
- Cornell, R.M. and U. Schwertmann. 2003. *The Iron Oxides: Structure, Properties, Reactions, Occurrences and Uses*. Wiley-VCH, Weinheim, Germany.
- Cornu, S., Y. Lucas, E. Lebon, J.P. Ambrosi, F. Luizao, J. Rouiller, M. Bonnay and C. Neal. 1999. Evidence of titanium mobility in soil profiles, Manaus, Central Amazonia. *Geoderma* 91: 281-295.
- Delvaux, B., A.J. Herbillon, J.E. Dufey and L. Vielvoye. 1990. Surface properties and clay mineralogy of hydrated halloysitic soil clays. I. Existence of interlayer specific sites. *Clay Miner.* 25: 129-139.
- Eswaran, H. and C.B. Wong. 1978. A study of a deep weathering profile on granite in Peninsular Malaysia. Part II. Mineralogy of the clay, silt and sand. *Soil Sci. Soc. Am. J.* 42: 144-158.
- Fontes, M.P.F. and S.B. Weed. 1991. Iron oxides in selected Brazilian Oxisols: I. Mineralogy. *Soil Sci. Soc. Am. J.* 55: 1143-1149.
- Gee, G.W. and J.W. Baulder. 1986. Particle size analysis, pp. 383-411. In: A. Klute, G.S. Campbell, R.D. Jackson, M.M. Mortland and D.R. Nielson, eds., *Methods of Soil Analysis, Part I. Physical and Mineralogical Methods*. SSSA, Madison, Wisconsin.
- Hart, R.D., R.J. Gilkes, S. Siradz and B. Singh. 2002. The nature of soil kaolins from Indonesia and Western Australia. *Clays Clay Miner.* 50: 198-207.
- Hart, R.D., W. Wiriyakitnateekul and R.J. Gilkes. 2003. Properties of soil kaolins from Thailand. *Clay Miner.* 38: 71-94.
- Hughes, J.C. and G. Brown. 1979. A crystallinity index for soils kaolins and its relation to parent rock, climate and soils maturity. *Eur. J. Soil Sci.* 30: 557-563.
- Hughes, J.C., R.J. Gilkes and R.D. Hart. 2009. Intercalation of reference and soil kaolins in relation to physico-chemical and structural properties. *Appl. Clay Sci.* 45: 24-35.
- Islam, M.R., R. Stuart, A. Risto and P. Vesa. 2002. Mineralogical changes during intense chemical weathering of sedimentary rocks in Bangladesh. *J. Asian Earth Sci.* 20: 889-901.
- Kabata-Pendias, A. and H. Pendias. 2001. *Trace Elements in Soils and Plants*, 3rd edition. CRC Press, New York.
- Kanket, W., A. Sudhiprakarn, I. Kheoruenromne and R.J. Gilkes. 2005. Chemical and crystallographic properties of kaolin from Ultisols in Thailand. *Clays Clay Miner.* 53: 478-489.
- Kautz, C.Q. and P.C. Ryan. 2003. The 10 angstrom to 7 angstrom halloysite transition in a tropical soil sequence, Costa Rica. *Clays Clay Miner.* 51: 252-263.
- Klug, H.P. and L.E. Alexander. 1974. *X-Ray Diffraction Procedures for Polycrystalline and Amorphous Materials*. Wiley and Sons.
- Lair, G.J., F. Zehetner, M. Hrachowitz, N. Franz, F. Maringer and M.H. Gerzabek. 2009. Dating of soil

- layers in a young floodplain using iron oxide crystallinity. *Quat. Geochronol.* 4: 260-266.
- Ma, C. and R.A. Eggleton. 1999. Surface layer types of kaolinite: a high resolution transmission electron microscope study. *Clays Clay Miner.* 47: 181-191.
- Mehra, O. and P. Jackson. 1960. Iron oxide removal from soils and clays in a dithionite-citrate-bicarbonate system buffered with sodium. *Clays Clay Miner.* 7: 317-327.
- Melo, V.F., B. Singh, C.E.G.R. Schaefer, R.F. Novais and M.P.F. Fontes. 2001. Chemical and mineralogical properties of kaolinite-rich Brazilian soils. *Soil Sci. Soc. Am. J.* 65: 1324-1333.
- Montes, C.R., A.J. Melfi, A. Carvalho, A.C. Vieira-Coelho and M.L.L. Formoso. 2002. Genesis, mineralogy and geochemistry of kaolin depositions of the Jari River, Amapá state, Brazil. *Clays Clay Miner.* 50: 494-503.
- Motta da, P.E.F. and N. Kämpf. 1992. Iron oxide properties as support to soil morphological features for prediction of moisture regimes in Oxisols of Central Brazil. *Z.Pflanzennähr. Bodenk.* 155: 385-390.
- Muggler, C.C., P. Buurman and J.D.J. van Doesburg. 2007. Weathering trends and parent material characteristics of polygenetic Oxisols from Minas Gerais, Brazil: I. Mineralogy. *Geoderma* 138: 39-48.
- National Soil Survey Center. 1996. Soil Survey Laboratory Methods Manual, Soil Survey Investigations Report No. 42, Version 3.0. Natural Resources Conservation Service. U.S. Department of Agriculture, Washington D.C.
- Navarrete, I.A., V.B. Asio, R. Jahn and K. Tsutsuki. 2007. Characteristics and genesis of two highly weathered soils in Samar, Philippines. *Aust. J. Soil Res.* 45: 153-163.
- Norrish, K. and J.T. Hutton. 1969. An accurate X-ray spectrographic method for the analysis of a wide range of geological samples. *Geochim. Cosmochim. Acta* 33: 431-453.
- Pei, Y.C., K.W. Ming, S.Y. Deng and S.C. Shyun. 2004. Kaolin minerals form Chinmen Island (Quemoy). *Clays Clay Miner.* 52: 130-137.
- Prasetyo, B.H. and R.J. Gilkes. 1994. Properties of iron oxides from red soils derived from volcanic tuff in west Java. *Aust. J. Soil Res.* 32: 781-794.
- Quantin, P. 1990. Specificity of the Halloysite-Rich Tropical and Subtropical Soils. In: 14th International Congress of Soil Science. Japan, Vol. 7 (IUSS).
- Rasmussen, C., A.D. Randy and J.S. Randal. 2010. Basalt weathering and pedogenesis across an environmental gradient in the southern Cascade Range, California, USA. *Geoderma* 154: 473-485.
- Rayment, G.E. and B.R. Higginson. 1992. Australian Laboratory Handbook of Soil and Water Chemical Methods: Australian Soil and Land Survey Handbook. Inkata, Melbourne, Australia.
- Schaefer, C.E.G.R., J.D. Fabris and J.C. Ker. 2008. Minerals in the clay fraction of Brazilian Latosols (Oxisols): a review. *Clay Miner.* 43: 137-154.
- Schulze, D.G. 1984. The influence of aluminium on iron oxides: VIII. Unit-cell dimensions of Al-substituted goethites and estimation of Al from them. *Clays Clay Miner.* 32: 36-44.
- Schwertmann, U. 1988. Goethite and hematite formation in the presence of clay minerals and gibbsite at 25°C. *Soil Sci. Soc. Am. J.* 52: 288-291.
- Schwertmann, U. and L. Carlson. 1994. Aluminium influence on iron oxides: XVII. Unit-cell parameters and aluminium substitution of natural goethites. *Soil Sci. Soc. Am. J.* 58: 256-261.
- Schwertmann, U. and A.J. Herbillon. 1992. Some aspects of fertility associated with the mineralogy of highly weathered soils, pp. 47-59. In: Myths and Science of Soils of the Tropics. Special Publication 29, SSSA, Madison, Wisconsin.
- Schwertmann, U. and N. Kämpf. 1985. Properties of goethite and hematite in kaolinitic soils of southern and central Brazil. *Soil Sci.* 139: 344-350.
- Schwertmann, U. and G. Pfab. 1996. Structural vanadium and chromium in lateritic iron oxide: genetic implications. *Geochim. Cosmochim. Acta* 60: 4279-4283.
- Schwertmann, U. and R.M. Taylor. 1989. Iron oxides, pp. 379-438. In: J.B. Dixon and S.B. Weed, eds., Minerals in Soil Environments. SSSA, Madison, Wisconsin.
- Singh, B. and R.J. Gilkes. 1991. Concentration of iron oxides from soil clays by 5 M NaOH treatment: the complete removal of sodalite and kaolin. *Clay Miner.* 26: 463-472.
- Singh, B. and R.J. Gilkes. 1992a. Properties of soil kaolins from South-Western Australia. *Eur. J. Soil Sci.* 43: 645-667.
- Singh, B. and R.J. Gilkes. 1992b. Properties and distribution of iron oxides and their association with minor elements in the soils of South-Western Australia. *Eur. J. Soil Sci.* 43: 77-98.
- Siradz, S. 2000. Mineralogy and Chemistry of Red Soils of Indonesia. Ph.D. Thesis. The University of Western Australia.
- Stiles, C.A., C.I. Mora and S.G. Driese. 2003. Pedogenic processes and domain boundaries in a Vertisol climosequence: from titanium and zirconium distribution and morphology. *Geoderma* 116: 279-299.
- Thanachit, S., A. Sudhiprakarn, I. Kheoruenromne and R.J. Gilkes. 2006. The geochemistry of soils on a catena on basalt at Khon Buri, northeast Thailand. *Geoderma* 135: 81-96.
- Trakoonyingcharoen, P., I. Kheoruenromne, A. Sudhiprakarn and R.J. Gilkes. 2006a. Properties of kaolins in red Oxisols and red Ultisols in Thailand. *Appl. Clay Sci.* 32: 25-39.
- Trakoonyingcharoen, P., I. Kheoruenromne, A. Sudhiprakarn and R.J. Gilkes. 2006b. Properties of iron oxides in red Oxisols and red Ultisols as affected by rainfall and soil parent material. *Aust. J. Soil Res.* 44: 63-70.

- Watanabe, T., F. Shinya and K. Takashi. 2006. Clay mineralogy and its relationship to soil solution composition in soils from different weathering environments of humid Asia: Japan, Thailand and Indonesia. *Geoderma* 136: 51-63.
- Wisawapipat, W., I. Kheoruenromne, A. Suddhiprakarn and R.J. Gilkes. 2009. Surface charge characteristics of variable charge soils in Thailand. *Aust. J. Soil Res.* 48: 337-354.
- Yoothong, K., L. Moncharoen, P. Vijarnson and H. Eswaran. 1997. Clay mineralogy of Thai soils. *Appl. Clay Sci.* 11: 357-371.
- Zhang, G.L., J.H. Pan, C.M. Huang and Z.T. Gong. 2007. Geochemical features of a soil chronosequence developed on basalt in Hainan Island, China. *Rev. Mex. Cienc. Geol.* 24: 261-269.

Manuscript received 30 October 2010, accepted 25 January 2011